

# Breakdown of Lindstedt Expansion for Chaotic Maps

Guido Gentile

*Dipartimento di Matematica, Università di Roma Tre, Roma I-00146, Italy*

Titus S. van Erp

*Laboratoire de Physique / Centre Européen de Calcul Atomique et Moléculaire,  
Ecole Normale Supérieure de Lyon, 46 allée d'Italie, 69364 Lyon Cedex 07, France*

In a previous paper of one of us [Europhys. Lett. 59 (2002), 330–336] the validity of Greene’s method for determining the critical constant of the standard map (SM) was questioned on the basis of some numerical findings. Here we come back to that analysis and we provide an interpretation of the numerical results by showing that no contradiction is found with respect to Greene’s method. We show that the previous results based on the expansion in Lindstedt series do correspond to the transition value but for a different map: the semi-standard map (SSM). Moreover, we study the expansion obtained from the SM and SSM by suppressing the small divisors. The first case turns out to be related to Kepler’s equation after a proper transformation of variables. In both cases we give an analytical solution for the radius of convergence, that represents the singularity in the complex plane closest to the origin. Also here, the radius of convergence of the SM’s analogue turns out to be lower than the one of the SSM. However, despite the absence of small denominators these two radii are lower than the ones of the true maps for golden mean winding numbers. Finally, the analyticity domain and, in particular, the critical constant for the two maps without small divisors are studied analytically and numerically. The analyticity domain appears to be an perfect circle for the SSM analogue, while it is stretched along the real axis for the SM analogue yielding a critical constant that is larger than its radius of convergence.

PACS numbers: 05.45.-a, 05.45.Ac, 45.10.Hj

## I. INTRODUCTION

The Taylor-Chirikov map [1, 2] or standard map (SM) is one of the best known nonlinear models showing the onset of chaos in Hamiltonian systems. It describes with some level of approximation many physical systems. Among these there are numerous applications to plasma-physics, in which field it was originally introduced. The SM is also exactly related to the time evolution of the “kicked rotor” and the equilibrium condition for a chain of masses superpositioned on a periodic potential. The latter is known as the Frenkel-Kontorova (FK) model. This model is of equally importance for solid state physics as the SM is for plasma physics. It has, e.g., been applied to Josephson junctions arrays, charge density waves and surface friction [3]. More importantly, due to the simplicity and, yet, their complex behavior, these minimalistic models have had an enormous impact for our understanding in complex phenomena such as non-linearity, chaos, quasi-periodicity, and commensurate-incommensurate transitions. Although now part of any text-book in nonlinear physics and studied extensively over many years, the SM and FK still bear many unsolved problems. The most intriguing one of these is the sudden transition from smooth to chaotic orbits in the SM when the coupling parameter  $K$  is increased above a critical value  $K_c$ . In the FK model this transition is connected to change from a sliding to a pinned state and bears the name Aubry- or *breaking analyticity*- transition.

The theoretical framework that characterizes this

transition originates from the Kolmogorov-Arnold-Moser (KAM) theorem [4] that deals with the problem of small denominators that can occur in any perturbation expansion for quasi-integrable systems. In fact, the KAM theorem can be used to prove the non-chaotic behavior of the SM for very small coupling  $K$  and sufficient irrational winding number  $l$ . Other arguments can then be applied to prove that a chaotic regime exists for values  $K > K'$  giving an upper bound to  $K_c$ . For  $l$  equal to the golden mean, there exists an analytical bound by Mather  $K_c < 4/3$  [5], and the computer assisted proof of MacKay and Percival  $K_c < 63/64 \approx 0.9844$  [6]. Moreover, another computer assisted analysis of Jungreis excluded the value  $K = 0.9718$  for possible occurrence of invariant circles (smooth orbits) [7].

There exist several methods to calculate  $K_c$  precisely, among which Greene’s method [2] has shown to be one of the most effective giving the estimate  $K_c = 0.971635$ . This method is based on the assumption that the dissolution of invariant curves can be associated with the sudden change from stability to instability of nearly closed orbits. The renormalization method of MacKay [8] is a further refinement of this method and has established the same value with higher digit precision with respect to the original Greene’s result. Yet, Greene’s hypothesis has only been partly proven. A result by Falcolini and de la Llave [9] asserts that the critical constants for symplectic maps can never be higher than the ones obtained by Greene’s method. Recently, the result has been extended to nontwist maps by Delshams and de la Llave [10]. Hence,  $K_c \leq 0.971635$  for the SM with the

golden mean as winding number.

Another way to calculate  $K_c$  is through the Lindstedt series expansion. The smooth orbits in the SM can be described by a continuous (analytic) periodic function beneath  $K_c$ . Hence, below  $K_c$  the Fourier spectrum of this function should be finite for each component while decaying to zero in the high frequency domain. Above  $K_c$  some divergence is expected: either infinitely high frequency components persist, or the amplitude of some components in the spectrum diverges, or both. By writing down the Taylor expansion and equating the Taylor orders in the functional equation satisfied by this conjugation function, the Fourier-Taylor components can, in principle, be derived from the ones of lower order. In Ref. [11] an evaluation of this expansion to high orders suggested a convergence to a value  $K_c \sim 0.97978$ , which is higher than Greene's result. In this article, we come back to this analysis and show that an apparent plausible assumption made in Ref. [11] is falsified beyond Taylor order  $n > 200$ . As a result, the Lindstedt expansion does not contradict Greene's result. The value  $K_c \sim 0.97978$ , however, does correspond to the critical value for a different map, the semi-standard map (SSM). We come back to this in Sec. III.

Aubry [12] proposed another method, that is probably not very effective for high precision evaluation in a computer algorithm, but still interesting. It is based on an eigenvalue calculation of the dynamical matrix for the FK chain close to the critical point. Although this, in principle, requires the diagonalization of an infinite matrix, one can use the fact that the eigenvector of the lowest mode tends to localize [13]. The instability of the FK chain can then be determined in successive approximants by calculating the determinants of finite matrices of increasing length.

Finally we mention the use of Padé approximants [38] to study numerically the entire analyticity domain. This is a powerful tool even if it is less precise than other methods for detecting the critical constant  $K_c$  and not completely under control from a rigorous point of view. It has, for instance, been employed in Ref. [14] and, very recently, in Ref. [15] where the existence of a natural boundary for the analyticity domain of the SM has been checked numerically. Always with the aim of studying the analyticity domain Falcolini and de la Llave [16] developed a variant of Greene's method working for complex values of the parameter  $K$  that gives an alternative to the Padé series approach.

Eventually, these approaches are assumed to converge to the same value. However, the proof of this is highly non-trivial. The ultimate goal, of course, would be to gain an analytical expression for  $K_c$ . This is still far beyond our capabilities. Inspired to investigate further the influence of the small denominators in the Lindstedt series expansion, we introduce two simplified models by setting rigorously all the denominators equal to one both for the SSM and the SM. In the latter case, this is a very well known model, Kepler's equation [17], which turns

out to have a very similar transition and can be solved analytically. The radius of convergence is found to be higher than the SM and SSM value in case of golden mean winding numbers.

This article is organized as follows: In Sec. II we introduce the SM and SSM. In Sec. III we come back to the analysis of Ref. [11] showing that the Lindstedt expansion does not violate Greene's method and make the comparison between the SM and SSM. In Sec. IV we present a new model in which we suppress the small denominators and give an analytical expression both for the radius of convergence and the critical constant. We end with conclusions in Sec. V.

## II. THE (SEMI-) STANDARD MAP

The SM and SSM are defined as

$$\begin{pmatrix} x_{i+1} \\ x_i \end{pmatrix} = \mathbb{T} \begin{pmatrix} x_i \\ x_{i-1} \end{pmatrix} = \begin{pmatrix} 2x_i + V'(x_i) - x_{i-1} \\ x_i \end{pmatrix}, \quad (1)$$

with

$$\begin{aligned} V'(x) &= \frac{K}{2\pi} \sin(2\pi x) && \text{for the SM,} \\ V'(x) &= \frac{K}{4\pi i} \exp(i2\pi x) && \text{for the SSM.} \end{aligned} \quad (2)$$

The resulting sequence  $(x_i \bmod 1)$  for  $i = 2, \dots, \infty$  originating from a starting point  $(x_1, x_0)$  produces a discrete trajectory on a two-dimensional torus. Such a trajectory for the SM can be related to the equilibrium positions of an infinite FK chain where particles with harmonic nearest neighbor coupling are placed on a periodic potential  $V(x) = K(2\pi)^{-2}(1 - \cos(2\pi x))$ . The SSM has not such a similar counterpart, but is much simpler in its mathematics. By definition,  $l \equiv \langle x_{i+1} - x_i \rangle$  is called the winding number or rotation number of the map. For low coupling  $K$  and  $l$  incommensurate to the periodicity of  $V'$ , there exists a continuous function  $g_l(x)$  such that the positions  $\{x_i\}$  can be expressed as

$$x_i = g_l(il + \alpha). \quad (3)$$

This function is often called the conjugating function or, in context with the FK model, the modulation or hull function. The subscript  $l$  indicates that the shape of the function depends on the rotation number. The conjugating function satisfies the functional equation

$$2g_l(x) - g_l(x+l) - g_l(x-l) = -V'(x + g_l(x)). \quad (4)$$

For  $K$  large enough the function  $g_l(x)$  becomes discontinuous. For the SM this implies that the orbits become chaotic and for the FK that the chain of particles gets pinned together with the appearance of a phonon gap. This transition, in context with the FK model, is also called analyticity breaking transition or Aubry transition.

There are several quantities of interest which one can introduce in order to study the transition from regular to

chaotic dynamics. As the function  $g_l(x)$  is analytic for  $K$  close to the origin one can consider its series expansion in powers of  $K$

$$g_l(x) = \sum_{n=1}^{\infty} K^n g_l^n(x), \quad (5)$$

and define the radius of convergence  $\rho(l)$  as

$$\rho(l) = \inf_{x \in [0,1]} \left( \limsup_{n \rightarrow \infty} |g_l^n(x)|^{1/n} \right)^{-1}, \quad (6)$$

where  $\inf_{x \in [0,1]}$  denotes the infimum or greatest lower bound in the domain  $x \in [0, 1]$  for the quantity within the brackets  $(\dots)^{-1}$  and  $\limsup_{n \rightarrow \infty}$  is the supremum limit giving the highest value for  $|g_l^k(x)|^{1/k}$  of all  $k > n$  in the limit  $n \rightarrow \infty$ . Note that the infimum appears in the definition of the radius of convergence because each invariant curve is filled densely by any trajectory lying on it as a result of the incommensurate winding number. Hence, existence of the invariant curve itself requires the latter to be defined for all  $x \in [0, 1]$ .

The critical constant  $K_c(l)$  is defined as the (positive) real value  $K_c(l)$  such that for  $K > K_c(l)$  the conjugating function is not analytic any more [39]. It is believed that the analyticity domain of the conjugating function has a natural boundary: this means that  $g(K, x)$ , which is the modulation function  $g(x)$  at a value  $K$ , has a set of singularities in terms of  $K$  that form a closed curve around the origin in the complex plane. Hence, the radius of convergence  $\rho$  corresponds to the singularity closest to the origin, while the critical constant  $K_c$  corresponds to the intersection of this curve with the (positive) real axis. By definition one has  $K_c(l) \geq \rho(l)$ , so that by estimating the radius of convergence one finds a lower bound for the critical constant. Furthermore it is generally accepted that  $K_c(\tau) = \rho(\tau)$  for the golden mean  $\tau = (\sqrt{5} - 1)/2 \approx 0.618034$  [40]. It is also commonly believed (on the basis of numerical simulations and heuristic arguments) that  $K_c(l)$  has the highest value for the golden mean  $\tau$ . Moreover,  $K_c(l)$  is assumed the same for all values  $l \in \mathbb{Z}(\tau)$ , i.e. the values that can be written as  $l = m\tau + n$  with  $m, n$  integer numbers.

So far, the most accurate method to calculate  $K_c$  is based on Greene's method (also known as residue criterion). In this method the infinite trajectory  $\{x_i\}$  with irrational winding number  $l$  is approached by successive approximants  $j$ , which are periodic trajectories with rational winding numbers  $l_j = p_j/q_j$  and  $x_{i+q_j} \bmod 1 = x_i$ . Hence,  $q_j$  and  $p_j$  are at each level  $j$  two integer values giving a better estimate of  $l$  for each increment in  $j$  and  $l = \lim_{j \rightarrow \infty} l_j$ . These numbers can for instance be obtained using the continued fraction expansion of  $l$ . For  $l = \tau$  this results in the Fibonacci numbers ( $\tau \approx F_{j-1}/F_j$  with  $F_0 = F_1 = 1$  and  $F_j = F_{j-1} + F_j$  for  $j > 1$ ). Conclusively, the Greene's method tells how to construct the periodic orbits and to measure their stability by means of the *residue* that does not tend to zero any more for  $K > K_c$ .

Besides only partly proven, Greene's method has also some other limitations. For instance, this method does not work for other interesting models, as the SSM and Siegel's problem [18], where the construction of periodic orbits fails [41]. The best general alternative is the Lindstedt series expansion. This method is more generally applicable (it also works for the SSM), but is less accurate than Greene's method for the SM.

### III. THE LINDSTEDT SERIES EXPANSION

**Standard Map:** A way to study the transition is by means of the Lindstedt series, which is the expansion of the function  $g_l(x)$  both in Fourier and in Taylor series [42]. By defining the Fourier transform as

$$g_l(x) = \sum_{k=-\infty}^{+\infty} X_k e^{2\pi i k x} \quad \text{with inverse:}$$

$$X_k = \int_0^1 dx g_l(x) e^{-2\pi i k x}, \quad (7)$$

and expanding

$$X_k = K X_k^1 + K^2 X_k^2 + K^3 X_k^3 + \dots, \quad (8)$$

we end up with Fourier-Taylor coefficients  $X_k^n$ , where  $n$  is the Taylor index and  $k$  is the Fourier index. Now, using Eq. (4) we can relate the Fourier-Taylor coefficients of order  $n$  by the ones with lower Taylor index by [11]

$$\omega_k^2 X_k^n = \frac{i}{4\pi} \left\{ \delta_{1,k} - \delta_{-1,k} \right\} \delta_{1,n} + \frac{i}{4\pi} \sum_{m=1}^{\infty} \frac{(i2\pi)^m}{m!} \times$$

$$\sum_{n_1+n_2+\dots+n_m=n-1} \left\{ \sum_{k_1+k_2+\dots+k_m=k-1} X_{k_1}^{n_1} X_{k_2}^{n_2} \dots X_{k_m}^{n_m} \right.$$

$$\left. - (-1)^m \sum_{k_1+k_2+\dots+k_m=k+1} X_{k_1}^{n_1} X_{k_2}^{n_2} \dots X_{k_m}^{n_m} \right\}, \quad (9)$$

with

$$\omega_k^2 = \frac{1}{X_k} \int_0^1 dx (2g_l(x) - g_l(x+l) - g_l(x-l)) e^{-2\pi i k x}$$

$$= 2(1 - \cos(2\pi k l)) = (2 \sin(\pi k l))^2, \quad (10)$$

and where  $\sum_{n_1+n_2+\dots+n_m=n-1}$  implies a summation of all possible integers  $n_1, n_2, \dots, n_m$  with the constraint that  $\sum_{i=1}^m n_i = n - 1$ . There are ways to reduce the number of summations in Eq. (9). One possible way was proposed in Ref. [11] to construct an extended matrix  $P(n, k, m)$  defined as

$$P(n, k, m) = \frac{(2\pi i)^m}{m!} \sum_{n_1+n_2+\dots+n_m=n}$$

$$\left[ \sum_{k_1+k_2+\dots+k_m=k} X_{k_1}^{n_1} X_{k_2}^{n_2} \dots X_{k_m}^{n_m} \right]. \quad (11)$$

One can show that  $P(n, k, m) = 0$  if  $|k| > n$  or  $m > n$ . This gives rise to following recursive relations [11]:

$$\begin{aligned}
P(1, \pm 1, 1) &= \frac{\mp 1}{2\omega_1^2}, \tag{12} \\
P(n, k, 1) &= -\frac{1}{2}\omega_k^{-2} \sum_{m=1}^{n-1} \left[ P(n-1, k-1, m) \right. \\
&\quad \left. - (-1)^m P(n-1, k+1, m) \right], \\
P(n, k, m) &= \frac{1}{m} \sum_{n'=1}^{n-m+1} \sum_{k'=\max\{-n', k-n+n'\}}^{\min\{n', k+n-n'\}} \\
&\quad P(n', k', 1) P(n-n', k-k', m-1), \quad m > 1,
\end{aligned}$$

from which we can distract the Fourier-Taylor coefficients by

$$X_k^n = \frac{P(n, k, 1)}{2\pi i}. \tag{13}$$

The components of the  $P$  matrix are all real and obey the symmetry relation  $P(n, k, m) = (-1)^m P(n, -k, m)$ . Moreover, besides being zero for  $|k| > n$  and  $m > n$ , the matrix  $P(n, k, m)$  has zero values whenever  $k+n$  is odd. Hence,  $k = n, n-2, \dots, -n$  are the only nonzero elements of  $P$ .

The evaluation of Eqs. (12) is very efficient to evaluate  $X_k^n$  obtaining a Taylor order of approximately  $n = 200$ . To go beyond this limit, sufficient computer power and time is needed as both the computation time as the number of nonzero matrix elements increase with  $\sim n^3$ . Hence, memory can become a severe problem as the number of components that have to be stored can easily go beyond the maximum allowed allocation limit of the computing system. In this work, we finally reached the level  $n = 700$  (see Fig. 1) and we believe that going beyond this order is not very profitable for obtaining a more accurate evaluation of  $K_c$ . We come back to these results after addressing the small denominator problem that arises from Eq. (12).

From Eq. (10) and the second line in Eq. (12) one sees that even for irrational values of  $l$ , the terms  $\omega_k^{-2}$  can become arbitrarily high for some  $k$ . This effect is a typical example of the ‘small denominator problem’ that can strongly prevent the convergence of any perturbative series. In fact, it requires a stronger condition than irrationality such as a Diophantine condition [4]. Among all the irrational numbers, the golden mean  $\tau$  suffers the least from the small denominator problem and has therefore the highest convergence radius  $K_c$ . The golden mean is relatively difficult to approximate by rational numbers as those arising, for instance, from the continued fraction expansion (one can say that it is the ‘most irrational number’). As addressed above, the best approximants for the golden mean are given by the Fibonacci numbers:  $\tau = F_j/F_{j+1}$ . Therefore, the small denominators will be most dominant for  $k = F_j$ . From the exact relation

$F_{j-1} - F_j\tau = (-\tau)^{j+1}$ , one can show that for  $j \rightarrow \infty$

$$\frac{1}{\omega_{F_j}^2} \approx \frac{1}{4\pi^2} \left( \frac{1}{\tau^2} \right)^{j+1} \sim (2.618)^{j+1}. \tag{14}$$

However, we would like to stress that the small denominator problem is not the only mechanism causing the breakdown of the perturbative approach. This becomes evident in Sec. IV where we introduce the model that arises when we rigorously set  $\omega_k^{-2} = 1$  for all  $k$  in the series of Eq. (12). Clearly, this simplified expansion can not be affected by the small denominators. However, it still has a radius of convergence and a critical constant, as shown by the analytical solution. As the radius of convergence  $\rho$  of this simplified model is found to be lower than  $\rho(\tau) = K_c(\tau)$  for the SM, it proves that the golden mean winding numbers  $l \in \mathbb{Z}(\tau)$  are remarkably resistant to the problem of small denominators. The full analysis of this model is given in Sec. IV.

Coming back to the results of Fig. 1, we see that indeed the evolution of  $P(n, k, 1)$  makes sudden jumps at the Fibonacci numbers as expected from Eq. (14). Besides, deceptively the values  $n = k = F_n$  seems to determine the whole power law behavior of  $X_k^n$ , which is true till Taylor order  $n \sim 200$ . This assumption made in Ref. [11] allows for a further simplification of Eq. (12) by defining the reduced matrix  $Q(n, m) \equiv P(n, n, m)$  obeying the relations

$$\begin{aligned}
Q(1, 1) &= \frac{-1}{2\omega_1^2}, \\
Q(n, 1) &= -\frac{1}{2}\omega_n^{-2} \sum_{m=1}^{n-1} Q(n-1, m), \tag{15} \\
Q(n, m) &= \frac{1}{m} \sum_{n'=1}^{n-m+1} Q(n', 1) Q(n-n', m-1).
\end{aligned}$$

This set of equations make high order ( $\sim n = F_{20} = 10946$ ) evaluations accessible for computer calculations. At this order the value of the radius of convergence seems to stabilize near  $\rho = 0.97978$ , but this is still higher than the one obtained by Greene’s method. As consequence, validity of Greene’s method was questioned in the quoted paper [11].

The more elaborated calculations in this work show that the assumption made in Ref. [11] was actually wrong as shown by the high order behavior in Fig. 1. Still, we find that  $k = n$  gives the maximum for  $|P(n, k, 1)|$  whenever  $n$  is a Fibonacci number. However, the character of the evolution changes from being peaked to more smooth oscillations. Clearly, the line connecting  $|P(F_j, F_j, 1)|$  does no longer dominate the increment of  $P$ -matrix elements for  $n > 200$ . As  $|P(n, k_{\max}(n), 1)|^{1/n}$  shows local maxima for  $(n, k_{\max}) = (383, 377)$  and  $(n, k_{\max}) = (622, 610)$  just after  $F_{13}$  and  $F_{14}$ , we fitted the line  $\alpha_2 \lambda_2^n$  through these points. From this fit,  $\lambda_2 = 1.0248$ , the estimate for  $K_c \approx \lambda_2^{-1} = 0.9758$  is obtained. Although still higher than Greene’s value, it is already considerably lower than  $\rho = 0.97978$  obtained from Eqs. (15) for

$n = F_{20} = 10946$  [11]. Note that the latter approach of Ref. [11] for this lower approximant  $n = F_{14} = 610$ , as obtained from the line  $\lambda_1^n$  (See Fig. 1), would result in  $\rho \approx 1/\lambda_1 = 0.9817$ , still approximately 0.002 higher than the nearly converged value of  $\rho = 0.97978$ . Hence, a decay of 0.004 from 0.9758 at  $n = 622$  to 0.9716 at  $n \rightarrow \infty$  is not unlikely. As a consequence, contrary to the results of the restricted series (15), there is no proof that the full Lindstedt series (12) violates Greene's hypothesis. This also shows that further simplification of Eqs. (12) is not easily obtained and that an accurate evaluation of  $K_c$  based on the Lindstedt perturbation is severely demanding.

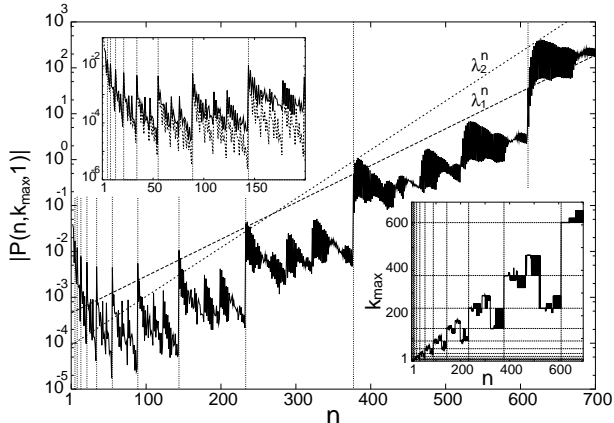


FIG. 1:  $|P(n, k_{\max}, 1)|$  as a function of  $n$ . This is defined as the maximum value of  $|P(n, k, 1)|$  of all  $k$ . Hence,  $k_{\max}$  is defined as the  $k$  value where  $|P(n, k, 1)|$  has this maximum. The inset in the lower corner shows  $k_{\max}$  as function of  $n$ . The inset in the left upper corner is an enlargement of the first 200 terms together with  $|P(n, n, 1)|$  (dashed line). From these figures, one can clearly detect sudden boosts in the function  $|P(n, k_{\max}, 1)|$  where  $k_{\max} = n$  at the Fibonacci values (dashed vertical lines). However, whereas for  $n < 200$  the character is sharply peaked at these values, its behavior changes for higher orders. Still  $k_{\max} = n$  for  $n$  a Fibonacci number, but the intersecting line described by  $\alpha_1 \lambda_1^n$  does no longer dominate the complete evolution of all the  $|P(n, k, 1)|$  terms.  $\lambda_1 = 1.0186$  is determined by the line through  $(n, k) = (F_{13}, F_{13}) = (377, 377)$  and  $(n, k) = (F_{14}, F_{14}) = (610, 610)$ .  $\lambda_2 = 1.0248$  is set by the line through  $(n, k) = (383, 377)$  and  $(n, k) = (622, 610)$  where  $|P(n, k_{\max}(n), 1)|^{1/n}$  shows local maxima in  $n$ . The inversed values,  $\lambda_1^{-1} \approx 0.9817$  and  $\lambda_2^{-1} \approx 0.9758$  are assumed to converge for higher  $n$  to  $K_c$  for the SSM and SM, respectively.

**Semi-Standard Map:** When evaluating Eq. (1) for the SSM (2), the factors  $\delta_{-1,k}$  and  $-(-1)^m \sum \dots$  are not present in Eq. (9). It is then straightforward to show that the  $P$ -matrix (11) has only non-zero elements for  $n = k$ . Hence, the assumption made in Ref. [11] that gave rise to Eqs. (15) does not correspond to the critical constant of the SM, but still gives the correct value for SSM. A result by Davie [19] shows that, for maps including the ones we are considering, the radius of convergence (6) is

equal to

$$\rho(l) = \left( \limsup_{n \rightarrow \infty} \max_{|k| \leq n} |X_k^n|^{1/n} \right)^{-1}. \quad (16)$$

Therefore, the radius of convergence for the SM cannot be larger than the radius of convergence of the SSM, but of course it implies only a lower bound on the critical constant. Numerically by using Padé approximants in Ref. [15] it has been found that for certain values of the rotation number  $l$ , the radius of convergence of the SM is strictly smaller than the radius for the SSM. For the golden mean it is hard to improve upon simple power series using Padé, but for other numbers closer to resonant values it is possible and the phenomenon becomes much more evident.

The fact that the critical constant for these numbers is lower for the SM than for the SSM implies, by (16), that dominant contributions arise from terms with Taylor orders  $n$  for which  $|X_{k_{\max}}^n| > |X_n^n|$ . This is exactly what emerges from the numerics as noted above and shown in Fig. 1 for  $n > 200$ . Clearly, this is not the case for the SSM where one can limit to  $k = n$ . Hence, in Ref. [11]  $K_c(\tau) = \rho(\tau)$  was actually determined for the SSM to be 0.97977 at Taylor order  $n = F_{20} = 10946$ . In the calculations of this work, we went to order  $n = F_{24} = 75025$ , that gave the value 0.97937. As the root criterion saturates very slowly, the numerical results provide essentially only an (accurate) upper bound for the radius of convergence.

To conclude this section, we found that, also for the golden mean, the radius of convergence for the SM is strictly less than the radius of convergence for the SSM. Therefore, as a general comment we can remark that for the SM the presence of all harmonics in the Fourier expansion of the coefficients  $g_l^n(x)$  has a double effect. On one hand the radius of convergence becomes smaller with respect to that of the SSM. On the other hand, the critical constant  $K_c(l)$  can be larger than its radius of convergence  $\rho(l)$  for  $l \notin \mathbb{Z}(\tau)$ . For the golden mean the two values are equal as emerges numerically [16], but for other values they can be appreciably different. One can imagine that the first phenomenon is due to the presence of contributions  $X_k^n$  larger than  $X_n^n$ , while the second one is a consequence of deep cancellations between the harmonics of given perturbative order. These two effects are, in general, much more dominant for rotation numbers  $l$  close to rational values (see for instance Refs. [15, 20, 21]).

#### IV. PUTTING SMALL DENOMINATORS TO UNITY

##### A. Introduction of the simplified maps

An interesting study appears if we set rigorously all possible small denominators equal to unity:  $\omega_k = 1$  for all  $k$  in Eqs. (12) and (15). Although the inspiration of

this model was simply to study of the perturbation expansion when the small denominators have no effect, we can retrace from this series back to a functional relation as the one in Eq. (4). It can be shown that these simplified series would correspond to the functional relation for a function  $h(x)$

$$h(x) + \frac{K}{4\pi i} \exp(i2\pi(x + h(x))) = 0 \text{ for the SSM and}$$

$$h(x) + \frac{K}{4\pi} \sin(2\pi(x + h(x))) = 0 \text{ for the SM.} \quad (17)$$

Hence, the divergence of the simplified series corresponds to the point in  $K$  where these functional forms (17) have no analytical solution any more. A logical next step would be to relate the equality (17) to the iteration of a map similar to Eq. (1). As the relation (17) does no longer contain the arguments  $x \pm l$  this is not so evident. However, one can relate the  $h(x)$  function to the hull function of a FK-type system. It can be shown that this corresponds to an one-dimensional Einstein solid that is interacting with an external incommensurate potential. Due to the lack of neighbor interaction, which makes each particle independent, it is highly unusual to describe for such a system the equilibrium coordinates by a collective hull function. Still, there are no restriction not to do so and one can even give such a function a physical meaning. As known from the FK model, the continuous shape of the hull function is directly associated with the existence of a sliding mode where the FK chain can slide over the periodic potential without cost of energy [3, 13]. In this case, the complete phonon spectrum is giving by sum of oscillations of the individual particles that are not zero in general. The sliding mode appears when we add an extra degree of freedom to the system as shown in Fig. 2.

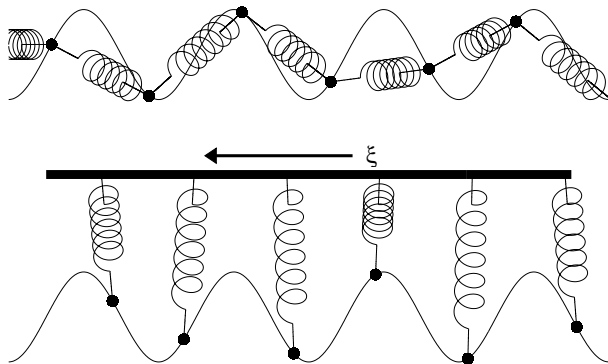


FIG. 2: Illustration of the FK model (top) and the system that obeys Eq. (17) (bottom). The latter corresponds also to the FKT model without neighbor interaction. All particle are connected to the upper rod whose position is given by  $\xi$ . A sliding mode may exist when  $\xi$  can be varied.

Here, all particles have no interaction to their neighbors, but are connected to an upper rod. When the rod has an infinite mass compared to the particle masses, the system is basically an Einstein solid. However, if we assume that the position of the rod may vary according to

a coordinate  $\xi$  an extra phonon mode exist that is zero for  $K < K_c$  in this system. Hence, the breakdown of the Lindstedt expansion (12) with  $\omega_k = 1$  for all  $k$  can be also related to a real physical sliding-pinning transition. The model as illustrated in Fig. 2 is also equal to a special case of the Frenkel-Kontorova-Tomlinson (FKT) model where each particle is connected to a rod by a spring with spring constant  $c_r$  and additionally to its neighbors with a coupling  $c_n$  [43]. The FKT model has been proposed to study more realistically the frictional behavior between atomic surfaces [22, 23, 24]. The model that is described by Eq. (17) simply corresponds to the FKT system with  $c_r = 1$  and  $c_n = 0$ . The nice thing is that the perturbation series of Eqs. (17) can be solved exactly. To show this, we will start with the more simple SSM case.

## B. Radii of convergence for simplified maps

**Simplified SSM:** It is convenient to use following normalization

$$R(n, m) = n!(-2)^n Q(n, m), \quad (18)$$

with matrix entries that are integer and positive and with  $R(n, n) = 1$ . From Eq. (12) and (18) with  $\omega_n^{-2} = 1$  we derive

$$R(n, 1) = n \sum_{m=1}^{n-1} R(n-1, m), \quad (19)$$

$$R(n, m) = \frac{1}{m} \sum_{n'=1}^{n-m+1} \binom{n}{n'} R(n', 1) R(n-n', m-1),$$

with  $\binom{n}{n'}$  the binomial coefficient:  $\equiv \frac{n!}{n'!(n-n)!}$ . Note that the recursive relations in Eq. (19) for  $m > 1$  coincide with those satisfied by the Stirling numbers of first and second kind,  $S_n^{(m)}$  and  $\mathfrak{S}_n^{(m)}$  respectively [44]. Of course what is different is the relation for  $m = 1$ .

From relations (19) with  $R(1, 1) = 1$  the following exact equality can be proven

$$R(n, m) = n^{n-m} \binom{n-1}{m-1}. \quad (20)$$

The proof of this equation is given in the appendix in two ways. In App. A1 we derive this proof using the argument of induction. In App. B1 we give a proof based on the tree formalism that was firstly introduced in Ref. [25]. The first proof is straightforward, but elongated. The second is short, but less self-contained as it requires some knowledge of the previous publications about the tree formalism. The latter is, however, most practical for the more complicated proof of relation for the SM in series of Eq. (17) with  $\omega_k^{-2} = 1$ . Now, from Eq. (18) and (20) we deduce that

$$Q(n, 1) = (-1)^n \frac{n^{n-1}}{2^n n!}, \quad (21)$$

which is assumed to increase as a power law  $\sim a\lambda^n$  giving the radius of convergence as  $\rho = 1/\lambda$ . Hence,

$$\ln |Q(n, 1)| = (n-1)\ln(n) - n\ln(2) - \ln(n!). \quad (22)$$

Then using [26]

$$\ln(n!) = \left(n + \frac{1}{2}\right)\ln n - n + \frac{1}{2}\ln(2\pi), \quad (23)$$

that is an refinement of the well known Stirling's formula  $\ln n! \approx n\ln n - n$ , we get

$$\begin{aligned} \ln |Q(n, 1)| &= n(1 - \ln(2)) - \frac{3}{2}\ln(n) - \frac{1}{2}\ln(2\pi) \\ \Rightarrow |Q(n, 1)| &\sim \frac{1}{\sqrt{2\pi n^3}} \left(\frac{1}{2}e\right)^n, \end{aligned} \quad (24)$$

yielding a radius of convergence  $\rho = 2/e \approx 0.735759$ . This value is less than the SSM value or SM value. This is a bit contra-intuitive, as one would expect that the possible occurrence of small denominators would give a lower  $\rho$ . Apparently, this does not happen for the golden mean. This can be understood by following reasoning. Although the small denominator factors  $\omega_k^{-2}$  can become arbitrary large for some  $k$  giving a boost to the series (12) and (15), at most values of  $k$  they will be considerable smaller than 1 resulting in an opposite effect. Hence, for the golden mean as winding number the latter effect seems to be more dominant yielding an even higher value for  $\rho$  than the case where all  $\omega_k^{-2}$  terms are equal to 1.

**Simplified SM:** The simplified SM considered in Eq. (17) is well known in celestial mechanics [17] after applying the following variable transformation. Write  $K/2 = -e$  and  $2\pi x = M$  where  $e$  is the eccentricity and  $M$  is the mean anomaly. Then the eccentric anomaly  $E = 2\pi(x + h(x))$  is related to  $M$  through Kepler's equation  $M = E - e \sin E$ , which is exactly the second equation in Eq. (17).

The recursive relations (12) with  $\omega_k^{-2} = 1$  have also an exact solution that we write here:

$$\begin{aligned} P(n, k, 1) &= \frac{(-1)^{n+(n-k)/2} k^{n-1}}{2^n ((n-k)/2)!((n+k)/2)!}, \\ &\text{for } |k| < n \text{ and if } k+n \text{ is even} \\ &= 0 \text{ otherwise,} \end{aligned} \quad (25)$$

which can be obtained by the Lagrange inversion theorem [17, 27]. We present a new derivation of this relation based on the tree formalism in the App. B 2

Then, by using Eq. (16) we see that we have to compute the maximum over  $k$  of  $|P(n, k, 1)|$ . By assuming that the maximum is reached for some  $k$  which is not too close to  $n$  (an assumption that we shall verify a posteriori [45]), we can approximate the factorial appearing in

Eq. (25) with Stirling's formula (23). This gives rise to

$$\begin{aligned} |P(n, k, 1)| &\sim \frac{1}{2^n} \frac{k^{n-1} e^n}{\left(\frac{1}{2}(n-k)\right)^{\frac{1}{2}(n-k)} \left(\frac{1}{2}(n+k)\right)^{\frac{1}{2}(n+k)}} \\ &\times \frac{1}{\left(\frac{1}{4}(n^2 - k^2)\right)^{\frac{1}{2}}} \\ &\sim \frac{2e^n}{n^2} \frac{1}{\sigma(1-\sigma^2)^{\frac{1}{2}}} \\ &\times \left( \frac{\sigma}{(1-\sigma)^{\frac{1}{2}(1-\sigma)}(1+\sigma)^{\frac{1}{2}(1+\sigma)}} \right)^n, \end{aligned} \quad (26)$$

where we have defined  $\sigma = k/n \in [-1, 1]$ . Hence, we have to compute the maximum of the function

$$E(\sigma) = \sigma \exp \left[ -\frac{1-\sigma}{2} \ln(1-\sigma) - \frac{1+\sigma}{2} \ln(1+\sigma) \right]. \quad (27)$$

By taking the derivative  $\frac{\partial E(\sigma)}{\partial \sigma} = 0$ , we find that the maximum is reached at a value  $\sigma_{\max}$  that satisfies following relation:

$$2 + \sigma_{\max} \ln(1 - \sigma_{\max}) - \sigma_{\max} \ln(1 + \sigma_{\max}) = 0, \quad (28)$$

yielding  $\sigma_{\max} \approx 0.833557$ . Hence,  $k_{\max} = \sigma_{\max} n \approx 0.833557n$ . Using Eq. (28),  $E(\sigma_{\max})$  simplifies to  $E(\sigma_{\max}) = \frac{1}{e} \frac{\sigma_{\max}}{\sqrt{1-\sigma_{\max}^2}}$ . Inserting this relation into Eq. (26) gives

$$|P(n, k_{\max}, 1)| \sim \frac{2}{n^2 \sigma_{\max}^2} \lambda^{n+1}, \quad (29)$$

with  $\lambda = \frac{\sigma_{\max}}{\sqrt{1-\sigma_{\max}^2}}$ . This yields a radius of convergence  $\rho = \lambda^{-1} \approx 0.662743$ , which is known as the Laplace limit [28]. This value is again smaller than the radius of convergence of the true SM (recall that for the golden mean the radius of convergence  $\rho(\tau)$  equals  $K_c(\tau)$ ). Moreover, similar to the true maps, this SM-analogue transition value  $\rho$  is lower than the one of the SSM.

### C. The critical constant and the analyticity domain

The argument above gives only information about the location of the singularities closest to the origin. The solution of the functional equations (17) could still exist for real values of  $K$  larger than the radius  $\rho$ . This is the situation  $K > \rho$  where  $h(K, x)$  is still analytical, but at which the power series (5) and (8) are no more defined. This is typical for a summation that consists of both positive as negative terms. In particular, there could be no singularity at all on the real axis so that an analytical form of  $h(K, x)$  could still exist for  $K \rightarrow \infty$ .

To analyze the extent of the analyticity domain and the critical constants, we need to 'evaluate' the summations

of Eqs. (8) and (7). This means that we need to find functional form  $h(K, x)$  that corresponds to the power series, but, contrary to the summation itself, can still be perfectly defined for  $|K| > \rho$ .

In the following analysis, we will show that the analyticity domains for the simplified maps are, like the for true maps, also constrained by a closed boundary. More precisely, we find that for fixed  $x$  there are only a few singularities, but the union over all  $x \in [0, 1]$  of such singularities reconstruct a closed curve surrounding the origin. Hence, outside this natural boundary there is no function  $h(K, x)$  that can be obtained by an analytic continuation of the power series around  $K = 0$ . Although very unlikely, this does not completely exclude the existence of a very different function, say  $\hat{h}(K, x)$ , that is defined outside this domain and obeys Eq. (17) and may even persist for  $K \rightarrow \infty$ . Recurrence phenomena of this kind are known to occur for certain maps [29], but, for instance, this is not the case of the SM.

**Simplified SSM:** As for this model,  $X_k(K) = X_k^k K^n$  we can directly writing down the summation of Eq. (5) for  $h(K, x)$  function:

$$h(K, x) = \sum_{k=1}^{\infty} X_k^k K^k e^{2\pi i k x}. \quad (30)$$

Inserting the expression (21) gives

$$\begin{aligned} h(K, x) &= \frac{1}{2\pi i} \sum_{k=1}^{\infty} (-1)^k \frac{k^{k-1}}{2^k k!} K^k e^{2\pi i k x} = \\ &= \frac{1}{2\pi i} \sum_{k=1}^{\infty} |Q(k, 1)| K^k e^{\pi i k (2x+1)} \end{aligned} \quad (31)$$

To find the full analyticity domain of  $h(K, x)$ , one basically has to fix a certain value for  $x$ , say  $x = x'$ , and search for the singularities in  $K$  of the function  $h(K, x')$  by e.g. using the Padé approximants method. Then, one has to repeat, in principle, this procedure for all possible values of  $x$  and collect the set of all singularities to construct the full analyticity domain. Finally, the radius of convergence  $\rho$  is then the complex singularity closest to the origin, while  $K_c$  is the smallest (positive) real singularity, if any.

Vice versa, we could also fix the argument  $\phi$  of the complex value  $K$ , such that  $K = |K|e^{i\phi}$ . The summation (31) will then be maximized for  $x = -(\frac{\phi}{2\pi} + \frac{1}{2})$ , where each term in the sum turns into a positive value. For these values of  $K$  and  $x$ , using the inclusion argument and the root criterion on the delimiting series, one can show that the radius of convergence is given by  $2/e$ . Hence, for each  $x$  there is one singularity at  $K = -\frac{2}{e}e^{-i2\pi x}$ , and the complete set over all  $x$  forms a natural boundary that is a circle around the origin.

Note that this is very different from the true maps. Although not proven, numerical studies (for instance Ref. [15] and references quoted therein) suggest that for the SM and SSM the function  $g(K, x)$  has for each value

of  $x$ , independent to its value, an infinite set of singularities forming the same (for each  $x$ ) natural boundary. Numerical analysis [15] shows that the natural boundary of the SSM is a circle, just as in this simplified model. This property appears to be true irrespective to the choice of  $l$  as long as it fulfills Diophantine condition [4]. For the SM with golden mean as winding number this curve resembles close to a circle, but not very smooth and slightly elongated (about 1%) along the imaginary axis [16].

**Simplified SM:** Taking the power series (8) for  $X_k$  for the simplified SM using Eq. (25) we have

$$\begin{aligned} X_k(K) &= \sum_{n=1}^{\infty} \frac{1}{2\pi i} P(n, k, 1) K^n \\ &= \frac{1}{2\pi i} \sum_{n=|k|, |k|+2, \dots}^{\infty} K^n \frac{(-1)^{n+(n-k)/2}}{2^n} \\ &\quad \times \frac{k^{n-1}}{((n-k)/2)!((n+k)/2)!}. \end{aligned} \quad (32)$$

Changing variables to  $j = (n - |k|)/2$  gives:

$$\begin{aligned} X_k(K) &= \frac{(-1)^k}{2\pi i k} \sum_{j=0}^{\infty} \frac{(-1)^j}{2^{2j+|k|} j! (j+|k|)!} (|k|K)^{2j+|k|} \\ &= \frac{(-1)^k}{2\pi i k} J_{|k|}(K|k|), \end{aligned} \quad (33)$$

with  $J_v(z)$  the Bessel function of the first kind [30, 31] defined (for integers  $v$ ) as

$$J_v(z) \equiv \sum_{j=0}^{\infty} \frac{(-1)^j}{2^{2j+v} j! (j+v)!} z^{2j+v}. \quad (34)$$

As these Bessel functions  $J_v(z)$  have no singularities in  $z$ , neither has  $X_k(K)$  in  $K$ . Therefore, the Fourier components do not give direct information about  $K_c$ . On the other hand, one can conclude from Eqs. (33) and (34) that  $|X_k(K)|$  is maximized for pure imaginary  $K$ , so that the radius of convergence is lying on the imaginary axis on a distance  $\rho$  from the origin. Here, the individual terms in Eq. (34) can not cancel as  $(-1)^j$  is then neutralized by  $x^{2j} \sim K^{2j} = (-1)^j |K|^{2j}$ . Hence, we expect to obtain the singularity equal to the radius of convergence for  $K$  along the imaginary axis.

We can now try to evaluate the Fourier series (7) for  $h(x)$ :

$$\begin{aligned} h(K, x) &= \sum_{k=-\infty}^{+\infty} \frac{(-1)^k}{2\pi i k} J_{|k|}(|k|K) \exp(2\pi i k x) \\ &= \sum_{k=1}^{\infty} \frac{(-1)^k}{\pi k} J_k(kK) \sin(2\pi k x). \end{aligned} \quad (35)$$

Further simplification is achieved by taking the derivative to  $x$  and searching the singularities in

$$h'(K, x) = \sum_{k=1}^{\infty} 2(-1)^k J_k(kK) \cos(2\pi k x) \quad (36)$$

instead of  $h(K, x)$ . This is allowed as the two problems are equivalent.

From the series (36) we can guess for which values of  $x$  the singularities will be  $K_c$  and  $\rho$  respectively. As  $J_k(kK)$  is positive for real values  $0 < K < 1$  (see p. 534 in [31], we need to compensate the  $(-1)^k$  term by  $\cos(2\pi kx)$ . This is achieved for  $x = \frac{1}{2}$  that reduces Eq. (36) to

$$h'(K, \frac{1}{2}) = 2 \sum_{k=1}^{\infty} J_k(kK), \quad (37)$$

which has the exact solution (see formula (1) at p. 615 in [31])

$$2 \sum_{k=1}^{\infty} J_k(kK) = \frac{K}{1-K}. \quad (38)$$

Hence,  $h'(K, \frac{1}{2})$  has a singularity at  $K = 1$ , yielding the critical constant  $K_c = 1$ , a well known result in celestial mechanics [17].

The complete analyticity domain can be found in Ref. [17], p. 219. In Fig. 3) we represent what can be obtained by using Padé approximants for some values of  $x$ . What emerges is that the function  $h(x, K)$  has for each value of  $x$  a pair of complex singularities closest to the origin symmetric with respect to the real axis. For  $x$  going from 0 to  $1/2$  such singularities move continuously from  $-1$  to  $1$  along two (symmetric) curves which pass through the points  $\pm i\rho$  at  $x = 1/4$  (see Fig. 3). Hence the entire set of singularities closest to the origin lies on a curve which is smooth except at  $K = \pm 1$ , where it has a discontinuity in its first derivative (cf. again Ref. [17], p. 219). An important feature is, however, that, as already noted in a similar context by Simon [32], a natural boundary in  $K$  for fixed  $x$  seems to appear only in the presence of small divisors. In fact, the latter give rise to the occurrence of sudden peaks yielding a pattern similar to lacunary series [33] for which natural boundaries can be proved to arise. Hence, these peaks seem to be responsible of the formation of the natural boundary as suggested by Prange (cf. again Ref. [32]).

## V. CONCLUSIONS

We showed by a numerical evaluation of the Lindstedt series up to order  $n = 700$  that a previously assumed violation of Greene's criterion was ungrounded. The assumption that allowed the restricted series (15) was falsified for orders  $n > 200$ . The resulting critical constant did not correspond to the SM, but is still true for the SSM. From our numerics, we conclude that, for the golden mean, the SSM critical constant is strictly higher than the SM. This seems to be generally true for all winding numbers, but is specifically difficult to proof for the golden mean where both constants are very close. Still, the numerics till order  $n = 700$  do not give a complete convergence. An evaluation that would compare to the

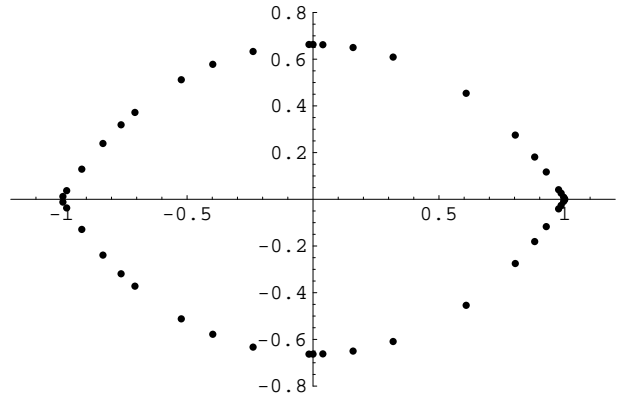


FIG. 3: Singularities in  $K$  of the function  $h(x, K)$  for the SM without small divisors for  $x$  varying in  $[0, 1]$ . The radius of convergence  $\rho$  corresponds to the value  $x = 1/4$ , while the critical constant  $K_c = 1$  corresponds to  $x = 1/2$ . The curve is symmetric with respect to both the real and the imaginary axes.

accuracy of Greene's method would rely on an prohibitive computational effort.

In addition to this analysis, we have purposed a new model that appears when the small denominators in the SM and SSM are suppressed. We show that this model maintains many features of the SM and SSM. However, it has an analytical solution and corresponds to Kepler's equation in case of the SM. Also here, the analogue of the SM has a lower value than the one of the SSM. Moreover, surprisingly the radii of convergence are lower than the true models for golden mean winding numbers. This proves that the golden mean winding numbers are remarkably resistant to the small denominator effect and falsifies a common misconception that the small denominator problem is the dominant and only mechanism for the breaking analyticity transition. The fact, that the simplified model still has a transition with a value even lower than the true maps for the golden mean, shows that this is not the case.

Finally, we studied the full analyticity domain for the two models. Also here, there are striking differences between the simplified- and the true maps. Similar to the true maps, the set of singularities form a natural boundary. However, whereas the SM and SSM all the singularities in  $K$  for the function  $g(K, x)$  are present for any value of  $x$ , the situation is different for the simplified maps. The simplified SSM has only one singularity in the complex  $K$ -plane for the function  $h(K, x)$  at each value of  $x$ . The simplified SM has for each value of  $x$  two singularities symmetric with respect to the real axis, except for the singularities on the real axis for  $x = 0$  and  $x = 1/2$ . The closed natural boundary is retained after gathering all singularities for all  $x$ .

This natural boundary is perfect circle in case of the

simplified SSM, while it is more stretched curve for the simplified SM with a discontinuity on the real axis at  $K = \pm 1$ . This shows that the radius of convergence of the simplified SSM equals its critical constant, like was found for the true maps with golden mean winding numbers. In contrast, the simplified SM has a critical constant of  $K_c = 1$  that is higher than its radius of convergence. In that respect, the simplified SM resembles more the true SM with winding numbers close to rational values. Also this is a bit of a surprise, as one would expect the contrary, but is consistent with the trend mentioned above. Somehow, it is almost as if the model, in which all small divisors were eliminated, still suffers more from this effect than the SM with the golden mean.

Therefore, we believe that the study of these kind of simplified analytical models are a worthy prerequisite for the understanding of the SM, SSM and FK models and, in particular, the influence of the small denominators.

### Acknowledgments

We thank Alberto Berretti for pointing out the relation between the simplified SM and Kepler's equation. T.S.v.E acknowledges the support by a Marie Curie Intra-European Fellowships (MEIF-CT-2003-501976) within the 6th European Community Framework Programme and the support through the European Network LOCNET HPRN-CT-1999-00163.

## APPENDIX A: INDUCTION PROOF

### 1. Proof of Eq. (20)

Assuming that relation (20) is true up to some Taylor order  $n-1$ , then the first relation of Eq. (19) for  $n$  yields:

$$\begin{aligned}
R(n, 1) &= n \sum_{m=1}^{n-1} \frac{(n-1)^{n-1-m}}{(m-1)!} \frac{(n-2)!}{(n-1-m)!} \\
&= n \sum_{m=0}^{n-2} \frac{(n-1)^m}{(n-2-m)!} \frac{(n-2)!}{m!} \\
&= n \sum_{m=0}^{n-2} (n-1)^m \binom{n-2}{m} \\
&= n((n-1)+1)^{n-2} = n^{n-1}, \tag{A1}
\end{aligned}$$

where in third equality we have used the binomial theorem

$$(1+x)^n = \sum_{j=0}^n \binom{n}{j} x^j. \tag{A2}$$

The second relation of Eq. (19) is more difficult. One can write

$$\begin{aligned}
R(n, m) &= \frac{1}{m} \sum_{n'=1}^{n-m+1} \binom{n}{n'} \binom{n-n'-1}{m-2} \\
&\times n'^{(n'-1)} (n-n')^{(n-n'-m+1)} \\
&= \frac{1}{m} \sum_{n'=1}^{n-m+1} \frac{n!}{n'!(n-n')!} \frac{(n-n'-1)!}{(m-2)!(n-n'-m+1)!} \\
&\times n'^{(n'-1)} (n-n')^{(n-n'-m+1)} \\
&= \frac{1}{m} \sum_{n'=1}^{n-m+1} \frac{n!}{n'!(m-2)!(n-n'-m+1)!} \\
&\times n'^{(n'-1)} (n-n')^{(n-n'-m)} \\
&= \frac{1}{m} \sum_{n'=1}^{n-m+1} \frac{n!}{(m-2)!(n-m+1)!} \binom{n-m+1}{n'} \\
&\times n'^{(n'-1)} (n-n')^{(n-n'-m)} \\
&= \frac{m-1}{m} \sum_{n'=1}^{n-m+1} \binom{n}{m-1} \binom{n-m+1}{n'} \\
&\times n'^{(n'-1)} (n-n')^{(n-n'-m)} \\
&= \frac{m-1}{m} \binom{n}{m-1} \sum_{n'=0}^{n-m} \binom{n-m+1}{n'+1} \\
&\times (n'+1)^{n'} (n-n'-1)^{(n-n'-1-m)} \\
&= \frac{(m-1)(n-m+1)}{m} \binom{n}{m-1} \sum_{n'=0}^{n-m} \binom{n-m}{n'} \\
&\times (n'+1)^{n'-1} (n-n'-1)^{(n-n'-1-m)}. \tag{A3}
\end{aligned}$$

Using Abel's identity [34]

$$\begin{aligned}
(x+y)(x+y-a\tilde{n})^{\tilde{n}-1} &= \sum_{k=0}^{\tilde{n}} \binom{\tilde{n}}{k} xy(x-ak)^{k-1} \\
&\times [y-a(\tilde{n}-k)]^{\tilde{n}-k-1}, \tag{A4}
\end{aligned}$$

with  $k = n'$ ,  $\tilde{n} = n - m$ ,  $a = -1$ ,  $x = 1$ ,  $y = m - 1$  yields

$$\begin{aligned}
mn^{n-m-1} &= \sum_{n'=0}^{n-m} \binom{n-m}{n'} (m-1) \\
&\times (1+n')^{n'-1} (n-n'-1)^{n-m-n'-1}. \tag{A5}
\end{aligned}$$

Hence

$$\begin{aligned}
R(n, m) &= \frac{(m-1)(n-m+1)}{m} \binom{n}{m-1} \sum_{n'=0}^{n-m} \binom{n-m}{n'} \\
&\times (n'+1)^{n'-1} (n-n'-1)^{(n-n'-1-m)} \\
&= (n-m+1) \binom{n}{m-1} n^{n-m-1} \\
&= \frac{n-m+1}{n} \frac{n!}{(m-1)!(n-m+1)!} n^{n-m} \\
&= \frac{(n-1)!}{(m-1)!(n-m)!} n^{n-m} = \binom{n-1}{m-1} n^{n-m}, \tag{A6}
\end{aligned}$$

## APPENDIX B: TREE FORMALISM

### 1. Proof of Eq. (20)

First of all, by defining  $\alpha = 2\pi x$  and  $u(\alpha) = 2\pi g(x)$ , one can write the functional relation that the function  $u(\alpha)$  has to satisfy as  $u(\alpha) + (K/2i) \exp(i\alpha + iu(\alpha)) = 0$  for the SSM and  $u(\alpha) + K \sin(\alpha + u(\alpha)) = 0$  for the SM. Note that in the case of the SSM the function  $u$ , which in principle depends on two parameters  $K$  and  $\alpha$ , is in fact a function of the only parameter  $\eta \equiv Ke^{i\alpha}$ .

In terms of the function  $u(\alpha)$  the functional equation (4) becomes, for the SM,

$$2u(\alpha) - u(\alpha + 2\pi l) - u(\alpha - 2\pi l) = -K \sin(\alpha + u(\alpha)), \tag{B1}$$

in which we recognize Eq. (1.4) of Ref. [20], with  $\varepsilon = K$  and  $\omega = l$ . For the SSM we have the same equation with the sine function replaced with  $(2i)^{-1} \exp(i\alpha + iu(\alpha))$ . Then we can envisage the same tree expansion as in Ref. [20]; see formula (2.2), where, to make a relation with the notations we are using now,  $k$  and  $\nu$  are what we are denoting with  $n$  and  $k$ , respectively. Moreover  $\gamma(nu_{\ell_v}) = -\omega_{\nu_{\ell_v}}$ , hence it is  $-1$  in our case, and one has  $\nu_v = 1$  for the SSM and  $\nu_u \in \{\pm 1\}$  for the SM. At the end we find

$$X_k^n = \frac{1}{2\pi i} \frac{(-1)^n}{2^n} \sum_{\vartheta \in \mathcal{T}_{n,k}} \text{Val}(\vartheta), \quad \text{Val}(\vartheta) = \prod_{u \in \vartheta} \frac{1}{m_u!} \nu_u^{m_u+1}, \tag{B2}$$

where the trees  $\vartheta$ , the branching numbers  $m_u$  and the set of trees  $\mathcal{T}_{n,k}$  of order  $n$  (that is with  $n$  nodes) and with momentum  $k$  flowing through the root line (that is such that  $\sum_{u \in \vartheta} \nu_u = k$ ) are defined as in Ref. [20].

In the case of the SSM, Eq. (B2) reduces to

$$X_n^n = \frac{1}{2\pi i} \frac{(-1)^n}{2^n} \sum_{\vartheta \in \mathcal{T}_{n,n}} \text{Val}(\vartheta), \quad \text{Val}(\vartheta) = \prod_{u \in \vartheta} \frac{1}{m_u!}, \tag{B3}$$

as  $\nu_u \equiv 1$ , and the sum over trees of order  $n$  can be written as a sum over all possible configurations of branching numbers  $\{m_u\}_{u \in \vartheta}$  with the constraint  $\sum_{u \in \vartheta} m_u = n-1$ :

indeed they are the only labels of the trees, and their values uniquely determine the elements of  $\mathcal{T}_{n,n}$ . Therefore we can rewrite  $X_n^n$  as

$$\begin{aligned}
X_n^n &= \frac{1}{2\pi i} \frac{(-1)^n}{2^n} \sum_{m_1 + \dots + m_n = n-1} \frac{1}{m_1! \dots m_n!} \\
&= \frac{1}{2\pi i} \frac{(-1)^n}{2^n} \frac{n^{n-1}}{n!}, \tag{B4}
\end{aligned}$$

where we have used the multinomial theorem

$$\sum_{m_1 + \dots + m_n = p} \frac{n!}{m_1! \dots m_n!} x_1^{m_1} \dots x_n^{m_n} = (x_1 + \dots + x_n)^p, \tag{B5}$$

which extends the binomial theorem to  $n > 2$ ; see [35], §24.1.3.

### 2. Proof of Eq. (25)

In the case of the SM, without small divisors, we can still use formula (B2), but now one can have  $\nu_u = \pm 1$ .

$$\begin{aligned}
X_k^n &= \frac{1}{2\pi i} \frac{(-1)^{n+(n-k)/2}}{2^n} \binom{n}{(n-k)/2} \\
&\sum_{m_1 + \dots + m_n = n-1} \frac{\nu_1^{m_1} \dots \nu_n^{m_n}}{m_1! \dots m_n!} \\
&= \frac{1}{2\pi i} \frac{(-1)^{n+(n-k)/2}}{2^n} \frac{k^{n-1}}{((n-k)/2)!((n+k)/2)!}, \tag{B6}
\end{aligned}$$

for  $k = n - 2p$ , with  $p = 1, \dots, n$ .

By using the definition Eq. (16) of radius of convergence, we see that we have to compute the maximum over  $k$  of  $|X_k^n|$ .

As  $k = \sum_{u \in \vartheta} \nu_u$  we see that, first,  $k$  can assume only the values  $-n, -n+2, -n+4, \dots, n-4, n-2, n$  (so that, in particular,  $(n \pm k)/2$  is even), and, second, in order to have a contribution to  $X_k^n$  we have to put  $(n-k)/2$  mode labels  $\nu_u$  equal to  $-1$  and the remaining  $(n+k)/2$  mode labels equal to  $1$ . Moreover for any tree  $\vartheta \in \mathcal{T}_{n,k}$  we can write

$$\prod_{u \in \vartheta} \nu_u^{m_u+1} = \left( \prod_{u \in \vartheta} \nu_u \right) \left( \prod_{u \in \vartheta} \nu_u^{m_u} \right) = (-1)^{(n-k)/2} \prod_{u \in \vartheta} \nu_u^{m_u}, \tag{B7}$$

which inserted into Eq. (B2) gives, by using again the multinomial theorem,

$$\begin{aligned}
X_k^n &= \frac{1}{2\pi i} \frac{(-1)^{n+(n-k)/2}}{2^n} \binom{n}{(n-k)/2} \\
&\sum_{m_1 + \dots + m_n = n-1} \frac{\nu_1^{m_1} \dots \nu_n^{m_n}}{m_1! \dots m_n!} \\
&= \frac{1}{2\pi i} \frac{(-1)^{n+(n-k)/2}}{2^n} \frac{k^{n-1}}{((n-k)/2)!((n+k)/2)!}, \tag{B8}
\end{aligned}$$

- 
- [1] B. V. Chirikov, Phys. Rep. **52**, 263 (1979).
- [2] J. M. Greene, J. Math. Phys. **20**, 1183 (1979).
- [3] L. M. Floria and J. J. Mazo, Adv. Phys. **45**, 505 (1996).
- [4] M. Tabor, *Chaos and Integrability in Nonlinear Dynamics: An introduction* (Wiley, New York, 1989).
- [5] J. N. Mather, Ergod. Theor. and Dynam. Sys. **4**, 301 (1984).
- [6] R. S. MacKay and I. C. Percival, Commun. Math. Phys. **98**, 469 (1985).
- [7] I. Jungreis, Ergod. Theor. and Dynam. Sys. **11**, 79 (1991).
- [8] R. S. MacKay, *Renormalisation in area preserving maps, Advanced Series in Nonlinear Dynamics* (World Scientific, Singapore, 1993).
- [9] C. Falcolini and R. de la Llave, J. Stat. Phys. **67**, 609 (1992).
- [10] A. Delshams and R. de la Llave, SIAM. J. Math. Anal. **31**, 1235 (2000).
- [11] T. S. van Erp and A. Fasolino, Europhys. Lett. **59**, 330 (2002).
- [12] S. Aubry, Physica D **7**, 240 (1983).
- [13] T. S. van Erp, A. Fasolino, O. Radulescu, and T. Janssen, Phys. Rev. B **60**, 6522 (1999).
- [14] A. Berretti, A. Celletti, L. Chierchia, and C. Falcolini, J. Stat. Phys. **66**, 1613 (1992).
- [15] A. Berretti, C. Falcolini, and G. Gentile, Phys. Rev. E **64**, 015202 (2001).
- [16] C. Falcolini and R. de la Llave, J. Stat. Phys. **67**, 645 (1992).
- [17] A. Wintner, *The analytic foundations of celestial mechanics* (Princeton University Press, Princeton, NJ, 1941).
- [18] C. L. Siegel, Ann. of Math. **43**, 607 (1942).
- [19] A. M. Davie, Nonlinearity **7**, 219 (1994).
- [20] A. Berretti and G. Gentile, J. Math. Pure Appl. **78**, 159 (1999).
- [21] A. Berretti and G. Gentile, Comm. Math. Phys. **220**, 623 (2001).
- [22] M. Weiss and F. J. Elmer, Phys. Rev. B **53**, 7539 (1996).
- [23] M. Weiss and F. J. Elmer, Z. Phys. B: Condens. Matter **104**, 55 (1997).
- [24] T. Gyalog and H. Thomas, Eur. Phys. Lett. **37**, 195 (1997).
- [25] G. Gallavotti, Comm. Math. Phys. **164**, 145 (1994).
- [26] D. Wells, *The Penguin Dictionary of Curious and Interesting Numbers* (Penguin Books, Middlesex, England, 1986).
- [27] E. T. Whittaker and G. N. Watson, *A course of modern analysis* (Cambridge University Press, Cambridge, 1997).
- [28] S. R. Finch, *Mathematical constants* (Cambridge University Press, Cambridge, 2003).
- [29] J. Wilbrink, Physica D **26**, 358 (1987).
- [30] I. S. Gradshteyn and I. M. Ryzhik, *Table of integrals, series, and products* (Academic Press, San Diego, 2000).
- [31] G. N. Watson, *A treatise on the theory of Bessel functions* (Cambridge University Press, Cambridge, 1944).
- [32] B. Simon, Ann. of Phys. **159**, 157 (1985).
- [33] Y. Katznelson, *An introduction to harmonic analysis, Cambridge Mathematical Library* (Cambridge University Press, Cambridge, 2004).
- [34] J. Riordan, *Combinatorial Identities* (Wiley, New York, 1979).
- [35] A. M. Abramowitz and I. A. Stegun, *Handbook of Mathematical functions* (Dover Publications, New York, 1972).
- [36] H. Poincaré, *Les méthodes nouvelles de la mécanique classique, Vol. III* (Gauthier-Villars, Paris, 1899).
- [37] G. A. Tomlinson, Philos. Mag. **7**, 905 (1929).
- [38] The  $(L, M)$ -Padé approximation for a function  $f(x)$  is given by the ratio of two polynomials,  $f(x) \approx P_L(x)/Q_M(x)$ , with  $P_L = p_0 + p_1x + \dots + p_Lx^L$  and  $Q_M = 1 + q_1x + \dots + q_Mx^M$ . Hence, the simple Taylor expansion of order  $n$  can be considered as a special case of the Padé series with  $L = n$  and  $M = 0$ .
- [39] The reason why one usually does not consider the negative critical constant, that is the negative value  $K'_c(l)$  such that for  $K < K'_c(l)$  there is no more an analytic orbit, is that  $K'_c(l) = -K_c(l)$  for the SM.
- [40] The golden mean is sometimes in other literature defined as the inverse of this value:  $(\sqrt{5}+1)/2 = \tau^{-1} \approx 1.618034$ .
- [41] One can easily check the non-existence of smooth periodic orbit by a first orders perturbation theory.
- [42] Such expansions were originally introduced by Lindstedt and Newcomb to study problems in celestial mechanics [36].
- [43] The simple Tomlinson model [37] is not the system in Fig. 2 as this usually consists of only one single oscillator (particle). This ancient model is now often applied to simulate the “stick-slip” motion of an atomic force microscope(AFM)-tip over a sample surface.
- [44] The Stirling numbers of the first kind  $S_n^{(m)}$  are defined by the requirement that  $(-1)^{n-m}S_m^{(n)}$  is the number of permutations of  $n$  symbols which have exactly  $m$  cycles. The Stirling numbers of the second kind  $\mathfrak{S}_n^{(m)}$  are equal to the way of partitioning a set of  $n$  elements into  $m$  non-empty subsets. See [35], p. 824, §24.1.3 and §24.1.4, with  $r = m - 1$ .
- [45] It is immediate to realize that the maximum is reached for some  $k \geq 1/2$ .